Available online at www.sciencedirect.com
ScienceDirect
Journal of Organometallic Chemistry 693 (2008) 1636–1644
Journal of Organometallic Chemistry
www.elsevier.com/locate/jorganchem

Facile cleavage of a phenyl group from $SbPh_3$ by dirhenium carbonyl complexes

Richard D. Adams *, Burjor Captain, William C. Pearl Jr.

Department of Chemistry and Biochemistry, University of South Carolina, Columbia, SC 29208, United States

Received 5 November 2007; received in revised form 15 November 2007; accepted 15 November 2007
Available online 22 November 2007

Dedicated to the memory of F.A. Cotton.

Abstract

The complex $Re_2(CO)_8[\mu\text{-}\eta^2\text{-}C(H){=}C(H)Bu^n](\mu\text{-}H)$ (**1**) reacts with $SbPh_3$ at 68 °C to yield the new σ-phenyl dirhenium complex $Re_2(CO)_8(SbPh_3)(Ph)(\mu\text{-}SbPh_2)$ (**4**) in 72% yield. Compound **4** contains two rhenium atoms held together by a bridging $SbPh_2$ ligand. One rhenium atom contains a σ-phenyl group. The other rhenium atom contains a $SbPh_3$ ligand. Compound **4** was also obtained in 34% yield from the reaction of $Re_2(CO)_{10}$ with $SbPh_3$ in the presence of UV–Vis irradiation together with some monorhenium products: $HRe(CO)_4SbPh_3$ (**5**), $Re(Ph)(CO)_4SbPh_3$ (**6**) and *fac*-$Re(Ph)(CO)_3(SbPh_3)_2$ (**7**) in low yields. Complex **4** is split by reaction with an additional quantity of $SbPh_3$ to yield the monorhenium $SbPh_3$ complexes **6**, **7** and *mer*-$Re(Ph)(CO)_3(SbPh_3)_2$ (**8**) that contain a σ-phenyl ligand. When **4** was treated with hydrogen, the phenyl ligand was eliminated as benzene and the dirhenium complexes $Re_2(CO)_8(\mu\text{-}SbPh_2)(\mu\text{-}H)$ (**10**), and $Re_2(CO)_7(SbPh_3)(\mu\text{-}SbPh_2)(\mu\text{-}H)$ (**11**), were formed that contain a bridging hydrido ligand. The doubly $SbPh_2$-bridged dirhenium complex $Re_2(CO)_7(SbPh_3)(\mu\text{-}SbPh_2)_2$ (**9**) that has no metal–metal bond was also formed in these two reactions.

Keywords: Rhenium; Antimony; Triphenylstibine; Phenyl group cleavage

1. Introduction

In recent studies, we have shown that the hexenyl-bridged dirhenium complex $Re_2(CO)_8[\mu\text{-}\eta^2\text{-}C(H){=}C(H)\text{-}Bu^n](\mu\text{-}H)$ (**1**) readily reacts with $HSnPh_3$ and $HGePh_3$ to yield the dirhenium complexes $Re_2(CO)_8(\mu\text{-}SnPh_2)_2$ (**2**) and $Re_2(CO)_8(\mu\text{-}GePh_2)_2$ (**3**) that contain two bridging $SnPh_2$ ligands or $GePh_2$ ligands, respectively, across a long rhenium–rhenium bond [1].

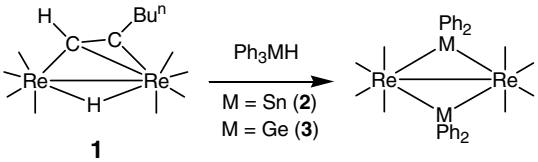

(1)

Cleavage of a phenyl ring from the $SnPh_3$ and $GePh_3$ groups of the $HSnPh_3$ and $HGePh_3$ molecules is required to form the bridging $SnPh_2$ and $GePh_2$ ligands, although no intermediates were observed in the formation of these products. However, in related studies, we have shown that the reactions of $HSnPh_3$ and $HGePh_3$ with certain polynuclear metal carbonyl complexes proceed by initial oxidative addition of the SnH or GeH bonds to metal cluster complexes containing a hydrido ligand and a $SnPh_3$ or $GePh_3$ ligand by a process that results in an opening of the cluster. When these compounds are heated, a phenyl ring is then cleaved from the $SnPh_3$ or $GePh_3$ ligand which then combines with a hydrido ligand and is eliminated as benzene and bridging MPh_2 ligands are formed in the cluster complexes, see Scheme 1, M = Ge, Sn [2].

Cleavage of phenyl groups from phosphine ligands is also well known in reactions of metal carbonyl complexes with PPh_3 and related ligands [3]. These processes often,

* Corresponding author. Tel.: +1 803 777 7187.
E-mail address: Adams@mail.chem.sc.edu (R.D. Adams).

0022-328X/$ - see front matter © 2007 Elsevier B.V. All rights reserved.
doi:10.1016/j.jorganchem.2007.11.028

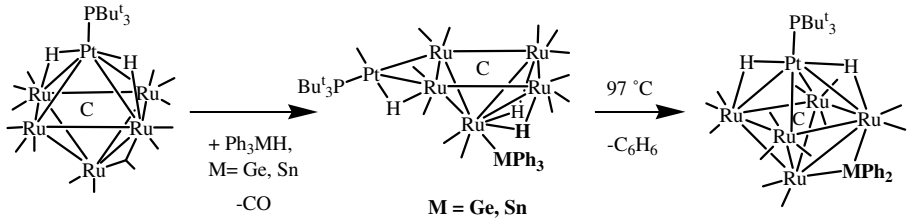

Scheme 1.

but not always, proceed by *ortho*-metalation of the phenyl ring. P–C bond cleavage may follow resulting in the formation of a bridging "benzyne" ligand. Leong et al. have shown that phenyl groups can also be cleaved from $SbPh_3$ in its reactions with triosmium and triruthenium carbonyl complexes [4]. Because of the similarities between $SbPh_3$ and $HSnPh_3$, we decided to examine the reactions of $SbPh_3$ with **1** and also with $Re_2(CO)_{10}$ under conditions of UV–Vis irradiation. These results are reported here. Cleavage of a phenyl ring from the $SbPh_3$ ligand to give products containing σ-coordinated phenyl groups is the dominant mode of reaction with these dirhenium compounds.

2. Experimental

2.1. General data

Reagent grade solvents were dried by the standard procedures and were freshly distilled prior to use. Infrared spectra were recorded on a Thermo Nicolet Avatar 360 FT-IR spectrophotometer. ^{1}H NMR spectra were recorded on a Varian Mercury 300 spectrometer operating at 300.1 MHz. Mass spectrometric (MS) measurements performed by a direct-exposure probe using electron impact ionization (EI) were made on a VG 70S instrument. Elemental Analyses were performed by Desert Analytics (Tucson, AZ). $SbPh_3$ and $Re_2(CO)_{10}$ were obtained from STREM and were used without further purification. $Re_2(CO)_8[\mu\text{-}\eta^4\text{-}C(H){=}C(H)Bu^n](\mu\text{-}H)$ was prepared according to a previously reported procedure [5]. Product separations were performed by TLC in air on Analtech 0.25 and 0.5 mm silica gel 60 Å F_{254} glass plates.

2.2. Reaction of $Re_2(CO)_8[\mu\text{-}\eta^4\text{-}C(H){=}C(H)Bu^n](\mu\text{-}H)$ (1) with $SbPh_3$

(a) At 68 °C: 104.5 mg (0.296 mmol) of $SbPh_3$ was added to 51.0 mg (0.07467 mmol) of $Re_2(CO)_8[\mu\text{-}\eta^4\text{-}C(H){=}C(H)Bu^n](\mu\text{-}H)$ in 80 mL of hexane. The reaction was heated to reflux for 3 h. The solvent was removed *in vacuo*, and the product was then isolated by TLC using a 4:1 hexane/methylene chloride solvent mixture. 70.0 mg (72% yield) of $Re_2(CO)_8(SbPh_3)(Ph)(\mu\text{-}SbPh_2)$ (**4**) was obtained. Spectral data for **4**: IR ν_{CO} (cm^{-1} in hexane): 2087(m), 2072(m), 2012(m), 2007(m), 1998(s), 1979(m), 1961(m), 1937(m), 1929(m). ^{1}H NMR (CD_2Cl_2, in ppm) $\delta = 7.08$–7.63 (m, 25 H, Ph), 6.77–6.94 (m, 5H, Ph–Re). Mass Spec. EI/MS *m/z*. 1302. The isotope pattern is consistent with the presence of two rhenium atoms and two antimony atoms. Elemental Anal. Calc.: C, 40.57; H, 2.32. Found: C, 40.51; H, 2.54%.

(b) At 25 °C: 53.1 mg (0.150 mmol) of $SbPh_3$ was added to 33.0 mg (0.0483 mmol) of $Re_2(CO)_8[\mu\text{-}\eta^4\text{-}C(H){=}C(H)\text{-}Bu^n](\mu\text{-}H)$ in 20 mL of hexane. The reaction was allowed to stir at room temperature for 24 h. The solvent was removed *in vacuo*, and the product was then isolated by TLC using a 4:1 hexane/methylene chloride solvent mixture to give 15.6 mg (25% yield) of **4**. A small amount of **1** (6%) was recovered from this reaction.

2.3. Photolysis of $Re_2(CO)_{10}$ with $SbPh_3$

$SbPh_3$ (104 mg, 0.2947 mmol) was added to a solution of $Re_2(CO)_{10}$ in 20 mL of benzene in a 100 mL three-neck flask equipped with a reflux condenser and a gas inlet. A slow stream of nitrogen was allowed to flow through the flask that was cooled to 0 °C and irradiated for 15 min. using a high pressure mercury UV lamp (American Ultraviolet Company, 1000 W) at the 250 wpi setting. The solvent was removed *in vacuo*, and the products were then isolated by TLC by using a 4:1 hexane/methylene chloride solvent mixture to yield in order of elution the following: 3.7 mg (4% yield) of colorless $HRe(CO)_4SbPh_3$, **5**, 5.7 mg (5% yield) of colorless $Re(Ph)(CO)_4SbPh_3$, **6**, 4.0 mg (3% yield) of colorless *fac*-$Re(Ph)(CO)_3(SbPh_3)_2$, **7**, and 31.7 mg (34% yield) of colorless **4**. Spectral data for **5**. IR ν_{CO} (cm^{-1} in hexane): 2080(w), 1992(m), 1979(s), 1964(m). ^{1}H NMR ($CDCl_3$, in ppm) $\delta = 7.30$–7.55 (m, 15H, Ph), −6.00 (s, 1H, hydride). Elemental Anal. Calc.: C, 40.51; H, 2.47. Found: C, 40.52; H, 2.50%. Spectral data for **6**. IR ν_{CO} (cm^{-1} in hexane): 2083(m), 1996(m), 1982(s), 1951(m). ^{1}H NMR (CD_2Cl_2, in ppm) $\delta = 7.20$–7.65 (m, 15H, Ph), 6.81–6.93 (m, 5H, Ph–Re). Elemental Anal. Calc.: C, 46.71; H, 2.77. Found: C, 45.93; H, 2.77. Spectral data for **7**. IR ν_{CO} (cm^{-1} in hexane): 2017(s), 1940(m), 1912(m). ^{1}H NMR (CD_2Cl_2, in ppm) $\delta = 7.12$–7.38 (m, 30H, Ph), 7.62 (m, 2H, Ph–Re), 6.68 (m, 1H, Ph–Re), 6.58 (m, 2H, Ph–Re). Mass Spec. EI/MS *m/z*. 1054. The isotope pattern is consistent with the presence of one rhenium atom.

2.4. Reaction of 4 with $SbPh_3$

$SbPh_3$ (90.2 mg, 0.256 mmol) was added to a solution of **4** (31.7 mg, 0.0243 mmol) in 20 mL of octane. The reaction

was heated to reflux for 3.5 h. The solvent was removed *in vacuo*, and the products were then isolated by TLC by using a 3:1 hexane/methylene chloride solvent mixture to yield in order of elution the following: 4.8 mg (14% yield) of **6**, 2.0 mg (4% yield) of *mer*-$Re(Ph)(CO)_3(SbPh_3)_2$ (**8**), 1.1 mg (3% yield) of $Re_2(CO)_7(SbPh_3)(\mu\text{-}SbPh_2)_2$ (**9**), 2.0 mg (4% yield) **7**, 9.7 mg (31% recovered) of **4**. Spectral data for **8**. IR ν_{CO} (cm^{-1} in hexane): 1933(s), 1910(m) cm^{-1}. ^1H NMR (CD_2Cl_2, in ppm) $\delta = 7.15$–7.67 (m, 30H, Ph), 6.52–6.93 (m, 5H, Ph–Re). Mass Spec. EI/MS *m/z*. 1054, M^+; 998, M^+-2CO. The isotope pattern is consistent with the presence of one rhenium atom. Spectral data for **9**: IR ν_{CO} (cm^{-1} in hexane): 2072(m), 2024(w), 2008(vw), 1987(s), 1981(s), 1955(s), 1937(s), 1928(m). ^1H NMR (CD_2Cl_2, in ppm) $\delta = 6.89$–7.74 (m, 35H, Ph). EI/MS *m/z*, 1474, M^+, 1446, M^+-CO, 1418, M^+-2CO, 1390, M^+-3CO. The isotope pattern is consistent with the presence of two rhenium atoms and three antimony atoms.

2.5. Reaction of 4 with H_2

Compound **4** (44.5 mg, 0.0342 mmol) was dissolved in 25 mL of octane. While purging with H_2 the reaction was heated to reflux for 6.25 h. The solvent was removed *in vacuo*, and the products were then isolated by TLC using 3:1 hexane/methylene chloride solvent mixture to yield in order of elution the following: 9.4 (31% yield) $Re_2(CO)_8(\mu\text{-}H)(\mu\text{-}SbPh_2)$ (**10**), 3.7 mg (9% yield) $Re_2(SbPh_3)(CO)_7(\mu\text{-}SbPh_2)(\mu\text{-}H)$ (**11**), 3.4 mg (7% yield) **9**. Spectral data for **10**: IR ν_{CO} (cm^{-1} in hexane): 2102(w), 2078(m), 2009(s), 1997(s), 1971(s) cm^{-1}. ^1H NMR (CD_2Cl_2, in ppm) $\delta = 7.35$–7.73 (m, 10 H, Ph), −16.341 (s, hydride, 1H). EI/MS *m/z*. 874, M^+, 846, M^+-CO. The isotope pattern is consistent with the presence of two rhenium atoms and one antimony atom. Spectral data for **11**: IR ν_{CO} (cm^{-1} in hexane): 2086(w), 2035(w), 2025(w), 1995(s), 1959(m), 1940(m), 1931(m) cm^{-1}. ^1H NMR ($CDCl_3$, in ppm) $\delta = 7.27$–7.80 (m, Ph, 25H), −16.00 (s, hydride, 1H). EI/MS *m/z*.1198, M^+, 1170, M^+-CO. The isotope pattern is consistent with the presence of two rhenium atoms and two antimony atoms.

2.6. Detection of benzene formation

A 4.8-mg amount of **4** was dissolved in 0.6 mL of toluene-d_8 in a 5 mm NMR tube. The NMR tube was evacuated and filled with H_2 five times. The NMR tube was heated in an oil bath at 100 °C for 3 h. After this period of time the NMR tube was taken out of the oil bath and cooled to room temperature to acquire an ^1H NMR spectrum. The ^1H NMR spectrum of this solution showed a singlet at $\delta = 7.13$ indicating the presence of benzene in solution.

2.7. Crystallographic analyses

Colorless single crystals of **4** suitable for X-ray diffraction analyses were obtained by slow evaporation of solvent from an octane/methylene chloride solvent mixture at room temperature. Colorless single crystals of **5**, **6**, **9**, **10** and **11** suitable for X-ray diffraction analyses were obtained by slow evaporation of solvent from a hexane/methylene chloride solvent mixture at −25 °C. Colorless single crystals of **7** and **8** suitable for X-ray diffraction analyses were obtained by slow evaporation of solvent from an octane/benzene solvent mixture at room temperature. Each data crystal was glued onto the end of a thin glass fiber. X-ray intensity data were measured by using a Bruker SMART APEX CCD-based diffractometer using Mo Kα radiation ($\lambda = 0.71073$ Å). The raw data frames were integrated with the SAINT+ program by using a narrow-frame integration algorithm [6]. Correction for Lorentz and polarization effects were also applied with SAINT+. An empirical absorption correction based on the multiple measurement of equivalent reflections was applied using the program SADABS. All structures were solved by a combination of direct methods and difference Fourier syntheses, and refined by full-matrix least-squares on F^2, using the SHELXTL software package [7]. All non-hydrogen atoms were refined with anisotropic displacement parameters. Hydrogen atoms were placed in geometrically idealized positions and included as standard riding atoms during the least-squares refinements. Crystal data, data collection parameters, and results of the analyses are listed in Tables 1–3.

Compounds **4**, **5**, **7**, **10** and **11** all crystallized in the triclinic crystal system. The space group $P\bar{1}$ was assumed

Table 1
Crystallographic data for compounds **4** and **5**

Compound	**4**	**5**
Empirical formula	$Re_2Sb_2O_8C_{44}H_{30}$	$ReSbO_4C_{22}H_{16}$
Formula weight	1302.58	652.30
Crystal system	Triclinic	Triclinic
Lattice parameters		
a (Å)	11.1865(4)	9.5987(6)
b (Å)	13.3720(5)	10.9613(7)
c (Å)	15.6059(6)	11.1779(7)
α (°)	93.979(1)	71.178(1)
β (°)	95.802(1)	86.402(1)
γ (°)	114.546(1)	84.894(1)
V ($Å^3$)	2096.51(14)	1108.04(12)
Space group	$P\bar{1}$ (#2)	$P\bar{1}$ (#2)
Z value	2	2
ρ_{calc} (g/cm^3)	2.063	1.955
μ (Mo Kα) (mm^{-1})	7.081	6.699
Temperature (K)	294(2)	294(2)
$2\Theta_{max}$ (°)	56.64	56.62
Number of observed ($I > 2\sigma(I)$)	8149	4720
Number of parameters	505	257
Goodness-of-fit (GOF)	1.036	1.044
Maximum shift in cycle	0.002	0.001
Residuals[a]: R_1; wR_2	0.0289; 0.0597	0.0312; 0.0639
Absorption correction, maximum/minimum	Multi-scan, 1.000/0.810	Multi-scan, 1.000/0.812
Largest peak in final difference in map ($e^-/Å^3$)	1.349	1.521

[a] $R = \sum_{hkl}(||F_{obs}| - |F_{calc}||)/\sum_{hkl}|F_{obs}|$; $R_w = [\sum_{hkl}w(|F_{obs}| - |F_{calc}|)^2/\sum_{hkl}wF_{obs}^2]^{1/2}$; $w = 1/\sigma^2(F_{obs})$; $GOF = [\sum_{hkl}w(|F_{obs}| - |F_{calc}|)^2/(n_{data} - n_{vari})]^{1/2}$.

Table 2
Crystallographic data for compounds **6**, **7** and **8**

Compound	**6**	**7**	**8**
Empirical formula	$ReSbO_4C_{28}H_{20}$	$ReSb_2O_3C_{45}H_{35}$	$ReSb_2O_3C_{45}H_{35}$
Formula weight	728.39	1053.43	1053.43
Crystal system	Monoclinic	Triclinic	Monoclinic
Lattice parameters			
a (Å)	16.9494(8)	10.4828(4)	12.5817(4)
b (Å)	12.0132(6)	11.0835(4)	21.1773(6)
c (Å)	13.6967(6)	19.2821(7)	15.2322(5)
α (°)	90	81.904(1)	90
β (°)	110.199(1)	87.127(1)	90.547(1)
γ (°)	90	66.110(1)	90
V (Å^3)	2617.4(2)	2027.9(1)	4058.4(2)
Space group	$P2_1/c$ (#14)	$P\bar{1}$ (#2)	$P2_1/n$ (#14)
Z value	4	2	4
ρ_{calc} (g/cm^3)	1.848	1.725	1.724
μ (Mo Kα) (mm^{-1})	5.683	4.337	4.334
Temperature (K)	294(2)	294(2)	294(2)
$2\Theta_{max}$ (°)	56.62	56.64	56.62
Number of observed ($I > 2\sigma(I)$)	5093	8086	8051
Number of parameters	307	460	460
Goodness of fit (GOF)	1.000	1.049	1.075
Maximum shift in cycle	0.002	0.001	0.002
Residuals[a]: R_1; wR_2	0.0264;0.0552	0.0357; 0.0694	0.0247; 0.0581
Absorption correction, maximum/ minimum	Multi-scan, 1.000/0.773	Multi-scan, 1.000/0.845	Multi-scan, 1.000/0.694
Largest peak in final difference Map (e$^-$/Å^3)	0.914	2.301	1.314

[a] $R = \sum_{hkl}(||F_{obs}| - |F_{calc}||)/\sum_{hkl}|F_{obs}|$; $R_w = [\sum_{hkl} w(|F_{obs}| - |F_{calc}|)^2/\sum_{hkl} w F_{obs}^2]^{1/2}$; $w = 1/\sigma^2(F_{obs})$; $GOF = [\sum_{hkl} w(|F_{obs}| - |F_{calc}|)^2/(n_{data} - n_{vari})]^{1/2}$.

Table 3
Crystallographic data for compounds **9**, **10** and **11**

Compound	**9**	**10**	**11**
Empirical formula	$Re_2Sb_3O_7C_{49}H_{35}$	$Re_2SbO_8C_{20}H_{11}$	$Re_2Sb_2O_7C_{37}H_{26}$
Formula weight	1473.42	873.44	1198.48
Crystal system	Orthorhombic	Triclinic	Triclinic
Lattice parameters			
a (Å)	18.9011(7)	12.1374(6)	8.8885(4)
b (Å)	22.0648(8)	13.9418(6)	11.1834(5)
c (Å)	22.5149(8)	16.1462(7)	19.3107(9)
α (°)	90	106.167(1)	102.5820(1)
β (°)	90	106.119(1)	97.6860(1)
γ (°)	90	100.181 (1)	90.629 (1)
V (Å^3)	9389.8(6)	2423.55(19)	1855.03(15)
Space group	$Pca2_1$ (# 29)	$P\bar{1}$ (#2)	$P\bar{1}$ (#2)
Z value	8	4	2
ρ_{calc} (g/cm^3)	2.085	2.394	2.146
μ (Mo Kα) (mm^{-1})	6.890	11.110	7.990
Temperature (K)	294(2)	294(2)	294(2)
$2\Theta_{max}$ (°)	50.06	52.04	52.04
Number of observed ($I > 2\sigma(I)$)	12344	6665	5649
Number of parameters	1090	565	427
Goodness of fit (GOF)	1.011	0.991	1.081
Maximum shift in cycle	0.003	0.001	0.000
Residuals[a]: R_1; wR_2	0.0351; 0.0684	0.0401; 0.0908	0.0454; 0.0830
Absorption correction, maximum/ minimum	Multi-scan, 1.000/ 0.733	Multi-scan, 1.000/0.107	Multi-scan, 1.00/0.505
Largest peak in final difference map (e$^-$/ Å^3)	1.452	1.377	1.123

[a] $R = \sum_{hkl}(||F_{obs}| - |F_{calc}||)/\sum_{hkl}|F_{obs}|$; $R_w = [\sum_{hkl} w(|F_{obs}| - |F_{calc}|)^2/\sum_{hkl} w F_{obs}^2]^{1/2}$; $w = 1/\sigma^2(F_{obs})$; $GOF = [\sum_{hkl} w(|F_{obs}| - |F_{calc}|)^2/(n_{data} - n_{vari})]^{1/2}$.

and confirmed by the successful solution and refinement for each of the structures. For compound **10** there were two independent molecules present in the asymmetric unit. The hydride ligand was located along the Re–Re bond in each molecule and they were refined on their positional parameters with a fixed isotropic thermal parameter. One of the phenyl rings (C61–C66) in the structural analysis of compound **11** was disordered over two orientations. It was refined in 50/50 disorder model with isotropic thermal parameters. The hydride ligand was located, and was refined by using geometric restraints (a fixed Re–H bond distance of 1.75 Å) and an isotropic thermal parameter.

Compounds **6** and **8** crystallized in the monoclinic crystal system. The space groups $P2_1/c$ and $P2_1/n$, respectively were identified uniquely on the basis of the systematic absences in the intensity data. Compound **9** crystallized in the orthorhombic crystal system. The systematic absences were consistent with either of the space group $Pca2_1$ or *Pbcm*. The structure could only be solved in the former space group. With $Z = 8$ there are two independent molecules present in the asymmetric unit. During the final stages of refinement atoms C12 and C42A had negative anisotropic thermal parameters. These two atoms were subsequently refined with isotropic thermal parameters.

3. Results and discussion

Only one product $Re_2(CO)_8(Ph)(SbPh_3)(\mu\text{-}SbPh_2)$ (**4**) was obtained in 72% yield from the reaction of **1** with $SbPh_3$ in hexane solution by heating to reflux for 1 h see Scheme 2.

The same product was obtained at 25 °C, but the yield was much lower, 25% after 24 h. Compound **4** was characterized by a combination of IR, ^{1}H NMR, mass spectral and single-crystal X-ray diffraction analyses. An ORTEP diagram of the structure **4** is shown in Fig. 1. The crystal of **4** contains one complete formula equivalent in the asymmetric crystal unit. The molecule contains the two rhenium atoms that are bridged by a $SbPh_2$ ligand. The rhenium atoms are not mutually bonded, Re(1)···Re(2) = 4.785(1) Å. The Re–Re bonding distance in $Re_2(CO)_{10}$ is 3.042(1) Å [8]. The Re–Re bond distance in **2** is

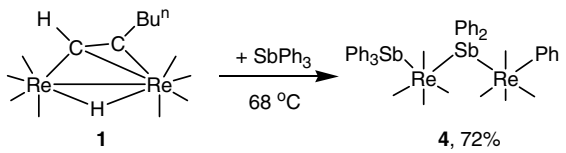

Scheme 2.

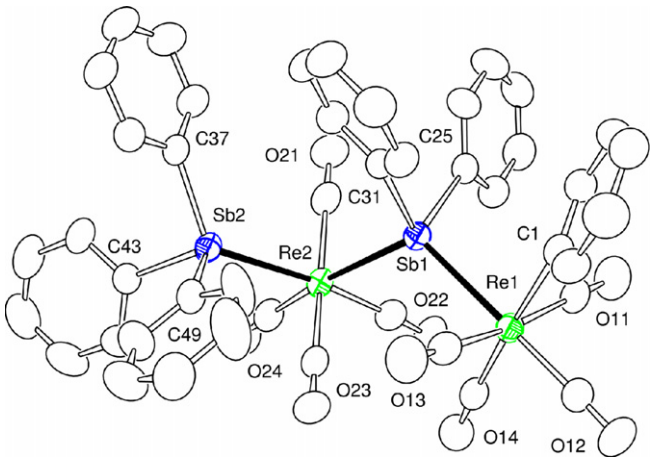

Fig. 1. An ORTEP diagram of the molecular structure of $Re_2(CO)_8(SbPh_3)(Ph)(\mu\text{-}SbPh_2)$ (**4**) showing 30% thermal ellipsoid probability. Selected interatomic bond distances (Å) and angles (°) are as follows: Re(1)...Re(2) = 4.785(1) Å, Re(1)–C(1) = 2.228(5), Re(1)–Sb(1) = 2.7676(4), Re(2)–Sb(2) = 2.7329(4), Re(2)–Sb(1) = 2.8159(4); C(1)–Re(1)–Sb(1) = 91.67(12), Sb(2)–Re(2)–Sb(1) = 101.176(11), Re(1)–Sb(1)–Re(2) = 117.96(1).

3.1685(3) Å in its monoclinic form and 3.1971(4) Å in a triclinic form [1]. The bridging $SbPh_2$ is slightly asymmetrical in its bonding to the two rhenium atoms, Re(1)–Sb(1) = 2.7676(4) Å and Re(2)–Sb(1) = 2.8159(4) Å. This could be due to steric effects since Re(2) contains a bulky $SbPh_3$ ligand in addition to the four terminal carbonyl ligands, while Re(1) has only the smaller σ-phenyl group with its four terminal carbonyl ligands. Both Re–Sb distances in **4** are slightly longer than those found for the bridging $SbPh_2$ ligand in the compound $Re_2(CO)_7(SbPh_3)(\mu\text{-}PPh_2)(\mu\text{-}SbPh_2)$ (**12**), Re–Sb = 2.748(2) Å and Re(2)–Sb(1) = 2.731(1) Å, which contains two ligands bridging the two metal atoms [9]. Compound **4** contains one $SbPh_3$ ligand coordinated to the metal atom Re(2). The Re–Sb distance is slightly shorter, Re(2)–Sb(2) = 2.7329(4) Å, than those of the bridging $SbPh_2$ ligand, but it is longer than the Re–Sb bond distance to the $SbPh_3$ ligand in **12**, Re–Sb = 2.671(1) Å [9]. The Re–C distance to the phenyl ring, Re(1)–C(1) = 2.228(5) Å, is only slightly longer than the Re–C distance to the phenyl ring in the compound $(C_5Me_5)Re(CO)_2I(Ph)$, 2.191(5) Å [10].

Compound **4** was also the major product obtained from the reaction of $SbPh_3$ with $Re_2(CO)_{10}$ in the presence of UV–Vis irradiation, but the yield was much lower, 34% yield. In addition to **4**, three minor products were obtained from this reaction, see Scheme 3. These were identified as $HRe(CO)_4SbPh_3$, **5**, 5% yield; $Re(Ph)(CO)_4SbPh_3$, **6**, 3% yield and *fac*-$Re(Ph)(CO)_3(SbPh_3)_2$, **7**, 3% yield. Each of the new products was characterized by IR, ^1H NMR and a single crystal X-ray diffraction analysis.

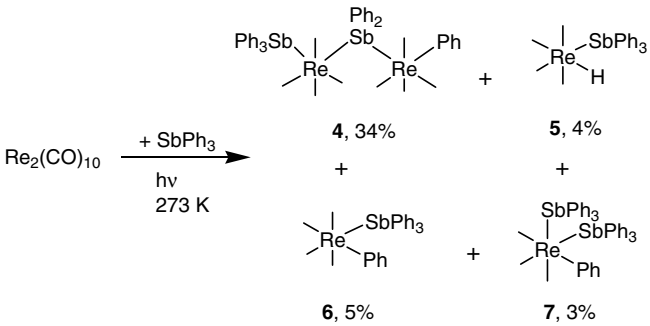

Scheme 3.

An ORTEP diagram of the molecular structure of **5** is shown in Fig. 2. Compound **5** contains only one rhenium atom. It has four terminal carbonyl ligands, one $SbPh_3$ ligand and a hydride ligand, H(1). The source of the hydride ligand has not been identified. The Re–Sb distance is similar to that found to the $SbPh_3$ ligand found in compound **4**, Re(1)–Sb(1) = 2.6931(4) Å. The hydrido ligand was located and refined crystallographically. It is positioned *cis* to the $SbPh_3$ ligand and it exhibits the usual characteristic high field resonance shift in its ^1H NMR spectrum, $\delta = -6.00$. The Re–H bond distance, Re(1)–H(1) = 1.78(5) Å, is similar to the Re–H bond distances that were observed in the related phosphine compounds, *fac*-$Re(H)(CO)_3[Ph_2P(CH_2)_3PPh_2]$, 1.70(4) Å [11]; *fac*-$Re(H)(CO)_3[Ph_2P(CH_2)_4PPh_2]$, 1.75(4) Å [11]; $Re(H)(CO)_4P(OMe)Ph_2]$, 1.60(8) Å [12] and *mer*-$Re(H)(CO)_3(P(OMe)Ph_2)_2$, 1.70(6) Å [12].

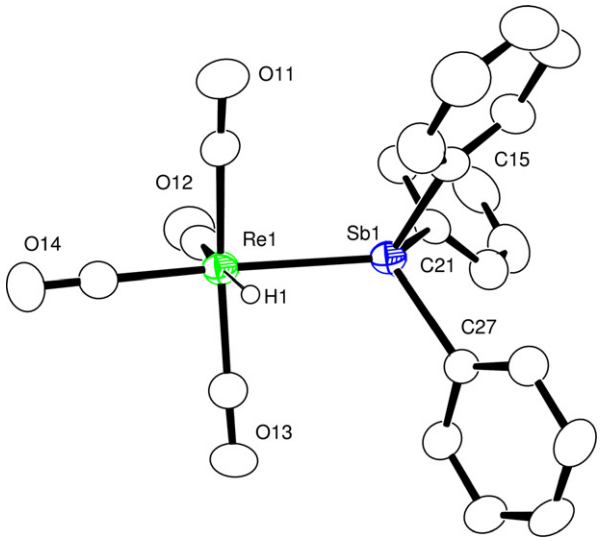

Fig. 2. An ORTEP diagram of the molecular structure of $HRe(CO)_4SbPh_3$ (**5**), showing 30% thermal ellipsoid probability. Selected interatomic bond distances (Å) and angles (°) are as follows: Re(1)–Sb(1) = 2.6931(4), Re(1)–H(1) = 1.78(5), Re(1)–C(14) = 1.952(5), Re(1)–C(12) = 1.965(5), Re(1)–C(11) = 1.981(5), Re(1)–C(13) = 1.987(5); Sb(1)–Re(1)–H(1) = 79.7(17).

An ORTEP diagram of the structure of **6** is shown in Fig. 3. Compound **6** is very similar to **5**. It contains only one rhenium atom, four terminal carbonyl ligands, one $SbPh_3$ ligand and a σ-phenyl ligand located *cis* to the $SbPh_3$ ligand. The Re–Sb distance is similar to that found in compounds **4** and **5**, Re(1)–Sb(1) = 2.7124(3) Å. The Re–C distance to the phenyl ring, Re(1)–C(15) = 2.226(4) Å, is very similar to the Re–C distance found in **4** and the compound $Cp^*Re(CO)_2(I)Ph$, [10].

Compound **7** is a $SbPh_3$ derivative of **6**. An ORTEP diagram of the structure of **7** is shown in Fig. 4. The three CO ligands have the *fac* structure. The Re–Sb distances are very similar to those in **4**, **5** and **6**, Re(1)–Sb(1) = 2.7176(4) Å, Re(1)–Sb(2) = 2.7151(3) Å. The Re–C distance to the phenyl ring is very similar to that in **6**, Re(1)–C(14) = 2.214(5) Å.

The reaction of **4** with $SbPh_3$ in an octane solution at reflux for 3.5 h provided compounds **6** and **7** in low yields, but also provided two new compounds *mer*-$Re(Ph)(CO)_3(SbPh_3)_2$ (**8**) in 4% yield and of $Re_2(CO)_7(SbPh_3)(\mu\text{-}SbPh_2)_2$ (**9**) in 3% yield. Thirty percent of the **4** was recovered after the 3.5 h reaction period.

An ORTEP diagram of the structure of **8** is shown in Fig. 5. Compound **8** is an isomer of **7**. The three CO ligands have a *mer* structure with the two $SbPh_3$ ligands occupying *trans*-coordination sites, Sb(1)–Re(1)–Sb(2) = 176.683(3)°. The Re–Sb distances are significantly shorter than those in **4**, **5** and **6**, Re(1)–Sb(1) = 2.6482(2) Å and Re(1)–Sb(2) = 2.6449(2) Å. The Re–C distance to the σ-bonded phenyl ring is similar to that in **6** and **7**, Re(1)–C(14) = 2.214(5) Å (see Scheme 4).

Compound **9** crystallizes with two independent molecules in the asymmetric crystal unit. Both molecules are structurally similar. An ORTEP diagram of the structure of one of two crystallographically independent molecules of **9** is shown in Fig. 6. Compound **9** is a dirhenium complex similar to **4**, but it contains two bridging $SbPh_2$ ligands. The Re–Re distance in **9**, Re(1)–Re(2) = 4.394(1) Å, Re(3)–Re(4) = 4.391(1) Å, is shorter than that in **4**, 4.785(1) Å, but much longer than that in **2**, 3.1685(3) Å (3.1971(4) Å) which contains a Re–Re bond [1]. In fact, both metals in **9** have 18 electron configurations on the basis of their ligand content, so there is no need to

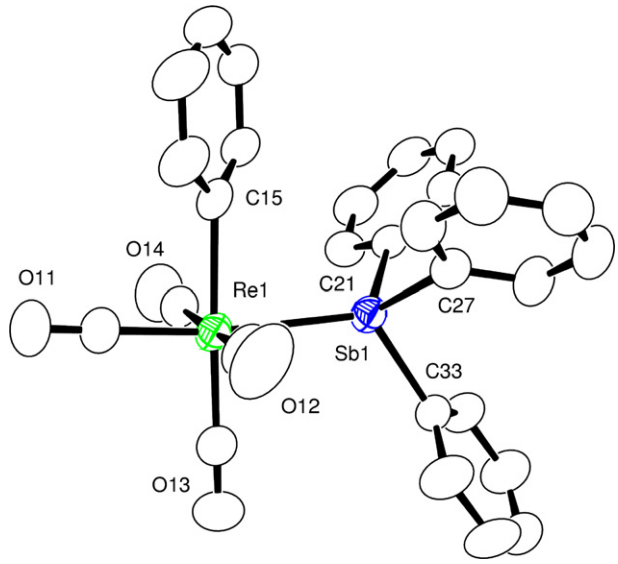

Fig. 3. An ORTEP diagram of the molecular structure of $Re(Ph)(CO)_4SbPh_3$ (**6**), showing 30% thermal ellipsoid probability. Selected interatomic bond distances (Å) and angles (°) are as follows: Re(1)–Sb(1) = 2.7124(3), Re(1)–C(15) = 2.226(4), Re(1)–C(14) = 1.984(4), Re(1)–C(12) = 1.984(4), Re(1)–C(11) = 1.929(4), Re(1)–C(13) = 1.952(5); Sb(1)–Re(1)–C(15) = 85.65(8).

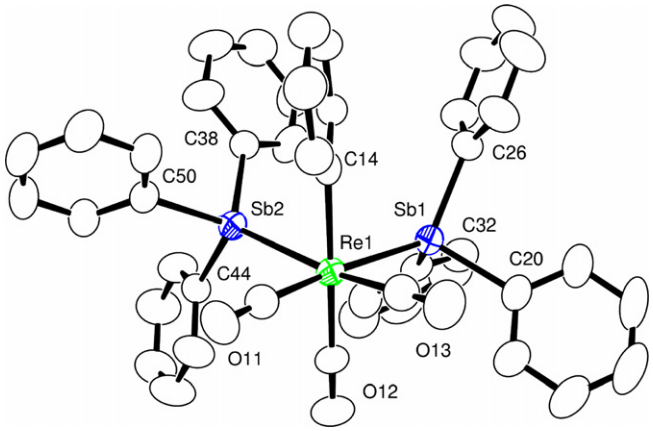

Fig. 4. An ORTEP diagram of the molecular structure of *fac*-$Re(Ph)(CO)_3(SbPh_3)_2$ (**7**), showing 30% thermal ellipsoid probability. Selected interatomic bond distances (Å) and angles (°) are as follows: Re(1)–Sb(1) = 2.7176(4), Re(1)–Sb(2) = 2.7151(3), Re(1)–C(14) = 2.214(5), Re(1)–C(12) = 1.950(5), Re(1)–C(11) = 1.914(5), Re(1)–C(13) = 1.922(6); Sb(1)–Re(1)–C(14) = 92.48(11), Sb(2)–Re(1)–C(14) = 83.33(11), Sb(1)–Re(1)–Sb(2) = 97.669(11).

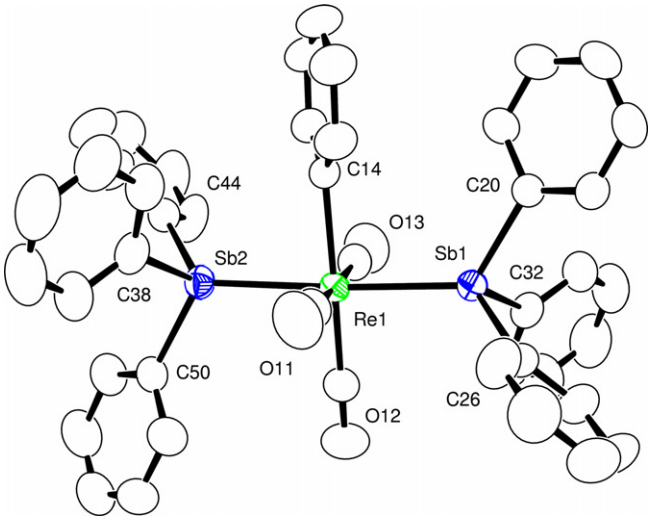

Fig. 5. An ORTEP diagram of the molecular structure of *mer*-$Re(Ph)(CO)_3(SbPh_3)_2$ (**8**), showing 30% thermal ellipsoid probability. Selected interatomic bond distances (Å) and angles (°) are as follows: Re(1)–Sb(1) = 2.6482(2), Re(1)–Sb(2) = 2.6449(2), Re(1)–C(14) = 2.230(3), Re(1)–C(12) = 1.940(4), Re(1)–C(11) = 1.967(4), Re(1)–C(13) = 1.980(4); Sb(1)–Re(1)–C(14) = 91.80(7), Sb(2)–Re(1)–C(14) = 84.99(7), Sb(1)–Re(1)–Sb(2) = 176.683(3).

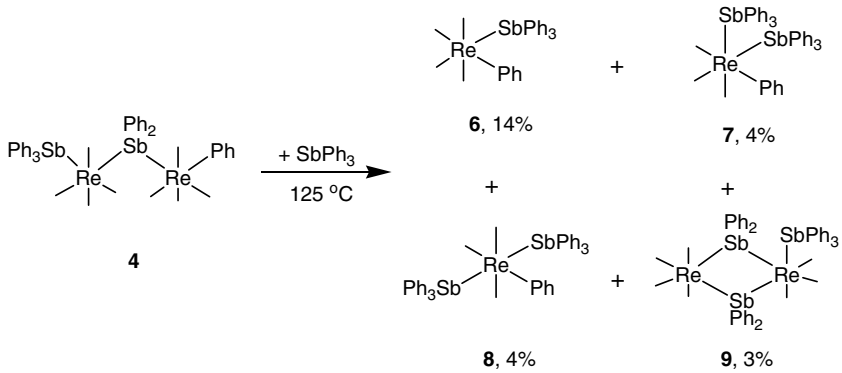

Scheme 4.

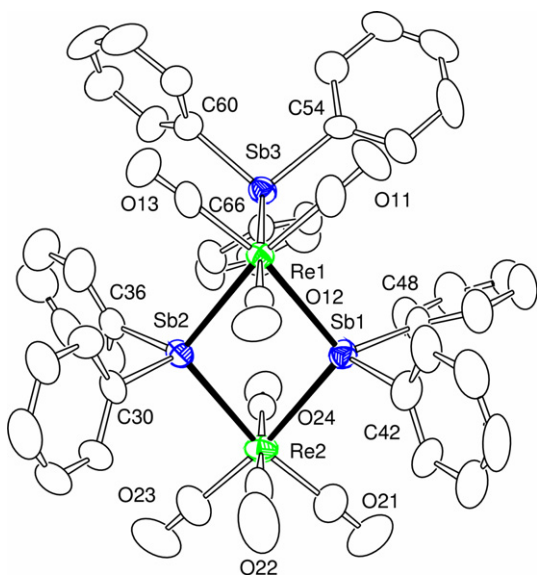

Fig. 6. An ORTEP diagram of the molecular structure of $Re_2(CO)_7(SbPh_3)(\mu\text{-}SbPh_2)_2$ (**9**), showing 30% thermal ellipsoid probability. Selected interatomic bond distances (Å) are as follows: Re(1)...Re(2) = 4.394(1), Re(3)...Re(4) = 4.391 (1), Re(1)–Sb(3) = 2.7412(18), Re(1)–Sb(2) = 2.7638(12), Re(1)–Sb(1) = 2.7670(13), Re(2)–Sb(2) = 2.7655(13), Re(2)–Sb(1) = 2.7772(13), Re(3)–Sb(5) = 2.7669(12), Re(3)–Sb(4) = 2.7753(12), Re(4)–Sb(6) = 2.7410(18), Re(4)–Sb(5) = 2.7546(12), Re(4)–Sb(4) = 2.7753(12).

expect the presence of a metal–metal bond. One rhenium atom in **9** has four CO ligands and the other rhenium atom has three CO ligands and one $SbPh_3$ ligand that lies *cis* to the two bridging $SbPh_2$ ligands. Compound **9** is structurally very similar to **12** [9]. The Re–Sb distances to the bridging $SbPh_2$ ligands Re(1)–Sb(2) = 2.7638(12) Å, Re(1)–Sb(1) = 2.7670(13) Å, Re(2)–Sb(2) = 2.7655(13) Å, Re(2)–Sb(1) = 2.7772(13) Å, Re(3)–Sb(4) = 2.7753(12) Å, Re(4)–Sb(5) = 2.7546(12) Å, Re(4)–Sb(4) = 2.7753(12) Å are similar to those **12**, 2.748(2) Å and 2.731(1) Å and in **4**, see above. The Re–Sb distances to the terminally coordinated $SbPh_3$ ligands are similar than those in **4**, **5**, **6**, **7** and **12**, Re(1)–Sb(3) = 2.7412(18) Å and Re(4)–Sb(6) = 2.7410(18) Å.

When hydrogen was purged through an octane solution of **4** at reflux for 3.5 h, three compounds were formed. These included **9** in a slightly higher yield 7%, and two new compounds **10** and **11** in 31% and 9% yields, respectively, see Scheme 5.

The coproduct benzene was observed spectroscopically (^{1}H NMR) when the reaction was performed under hydrogen in an NMR tube in d_8-toluene solvent at 100 °C. Compounds **10** and **11** were both characterized crystallographically. Compound **10** contains two crystallographically independent molecules in the asymmetric crystal unit. Both molecules are structurally similar. Compound **11** is simply a $SbPh_3$ derivative of **10**. ORTEP diagrams of the molecular structures of **10** and **11** are shown in Figs. 7 and 8, respectively. Both compounds contain two mutually bonded rhenium atoms that are bridged by a $SbPh_2$ ligand and a hydrido ligand. The Re–Re bond distances are 3.2244(6) Å [3.2396(5) Å] in **10** and 3.2574(5) Å in **11**. The slightly longer length of the Re–Re bond in **11** is probably due to steric interactions caused by the bulky $SbPh_3$ ligand on the atom Re(2). The Re–Re bond distance in the related phosphido complex $Re_2(CO)_8(\mu\text{-}PPh_2)(\mu\text{-}H)$ is slightly shorter at 3.165(1) Å, possibly because the phosphorus atom is smaller than the antimony atoms in **10** and **11** [13]. The Re–Sb bond distances to the bridging $SbPh_2$ ligand in **10** are slightly shorter than those in **4**

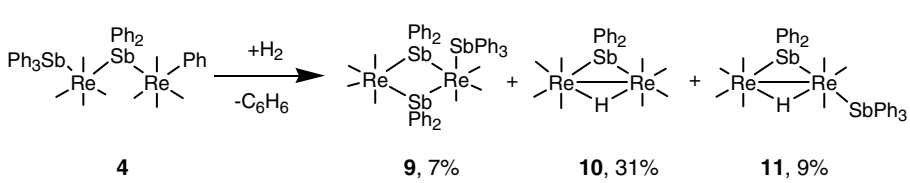

Scheme 5.

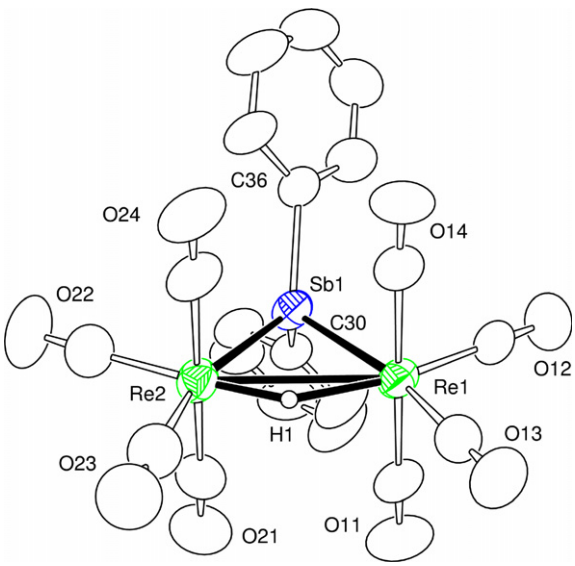

Fig. 7. An ORTEP diagram of the molecular structure of $Re_2(CO)_8(\mu\text{-}SbPh_2)(\mu\text{-}H)$ (**10**) showing 30% thermal ellipsoid probability. Selected interatomic bond distances (Å) and angles (°) are as follows: Re(1)–Re(2) = 3.2244(6), Re(1)–Sb(1) = 2.6934(7), Re(1)–H(1) = 1.98(7), Re(2)–Sb(1) = 2.6983(7), Re(2)–H(1) = 1.70(7), Re(3)–Sb(6) = 2.6983(8), Re(3)–Re(4) = 3.2396(5), Re(3)–H(2) = 2.00(7), Re(4)–Sb(6) = 2.6969(7), Re(4)–H(2) = 1.82(7).

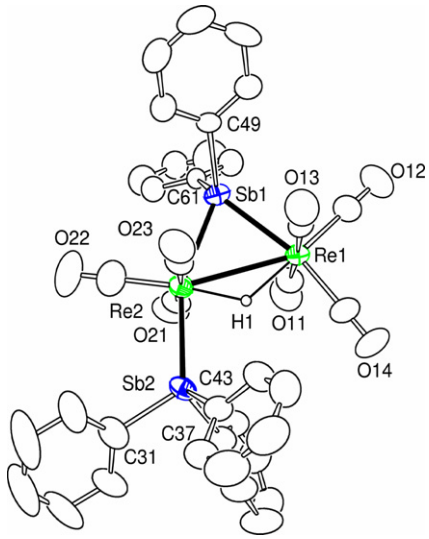

Fig. 8. An ORTEP diagram of the molecular structure of $Re_2(CO)_7(SbPh_3)(\mu\text{-}SbPh_2)(\mu\text{-}H)$ (**11**) showing 30% thermal ellipsoid probability. Selected interatomic bond distances (Å) and angles (°) are as follows: Re(1)–Re(2) = 3.2574(5), Re(1)–Sb(1) = 2.6948(7), Re(2)–Sb(1) = 2.6426(7), Re(2)–Sb(2) = 2.6430(7); Sb(1)–Re(2)–Sb(2) = 157.09(3).

and **9** and are nearly equal in length: Re(1)–Sb(1) = 2.6934(7) Å, Re(2)–Sb(1) = 2.6983(7) Å, [Re(3)–Sb(6) = 2.6983(8) Å, Re(4)–Sb(6) = 2.6969(7) Å]. In contrast, the Re–Sb bond distances to the bridging $SbPh_2$ ligand in **11** are significantly different, Re(1)–Sb(1) = 2.6948(7) Å, Re(2)–Sb(1) = 2.6426(7) Å with the shorter distance being associated with the rhenium atom that contains the bulky $SbPh_3$ ligand. The $SbPh_3$ ligand in **11** lies approximately *trans* to the short Re–Sb bond, Sb(1)–Re(2)–Sb(2) = 157.09(3)°. The shortness of the proximate Re–Sb bond is thus probably the result of a weaker structural *trans*-effect due to the different π-backbonding properties of the $SbPh_3$ ligand compared to that of CO ligands that lie trans to both Re–Sb bonds in **10** and in **11**. Compound **10** is structurally similar to the compound $Re_2(CO)_7(PPh_3)(\mu\text{-}PPh_2)(\mu\text{-}H)$ [14]. A similar structural *trans*-effect was observed in the Re–P bond distances involving the bridging PPh_2 ligand in this molecule. Compounds **10** and **11** both contain bridging hydrido ligands that lie opposite to the bridging $SbPh_2$ ligand. The hydrido ligand was located and refined in the structural analyses of **10**: Re(1)–H(1) = 1.98(7) Å, Re(2)–H(1) = 1.70(7) Å, [Re(3)–H(2) = 2.00(7) Å, Re(4)–H(2) = 1.82(7) Å]. The bridging hydrido ligand in **11** was located and refined with geometric constraints. As expected, both hydride ligands exhibit very high field resonance shifts in the ^1H NMR spectrum of the compounds: $\delta = -16.34$ for **10** and -16.00 for **11**.

4. Summary

It has been shown that a phenyl group is readily cleaved from $SbPh_3$ in its reactions with the rhenium carbonyl complexes **1** and $Re_2(CO)_{10}$. The novel σ-phenyl complex **4** was formed by insertion of a rhenium atom into the Sb–C(phenyl) bond. The rhenium–rhenium bond was also cleaved in the process. Interestingly, even in the reaction of $SbPh_3$ with **1** at room temperature, there was no evidence for formation of the compound $Re_2(CO)_8(SbPh_3)_2$, a likely intermediate in the formation of **4**, even though the bis-PPh_3 complex $Re_2(CO)_8(PPh_3)_2$ is stable and well known [14]. It must be that the Sb–C cleavage process is simply too facile even at this low temperature. The dirhenium complex **4** is split by reaction with an additional quantity of $SbPh_3$ to yield a series of monorhenium $SbPh_3$ complexes **6**–**8** containing a σ-phenyl ligand. When **4** was treated with hydrogen, the phenyl ligand was eliminated and the dirhenium complexes **10** and **11** were formed that contain a bridging hydrido ligands. The doubly $SbPh_2$-bridged dirhenium complex **9** that has no metal–metal bond was also formed in these two reactions.

Acknowledgement

This research was supported by the Office of Basic Energy Sciences of the US Department of Energy under Grant No. DE-FG02-00ER14980.

Appendix A. Supplementary material

CCDC 666183, 666184, 666185, 666186, 666187, 666188, 666189 and 666190 contain the supplementary crystallographic data for compounds **4**, **5**, **6**, **7**, **8**, **9**, **10** and **11**, respectively. These data can be obtained free of charge from The Cambridge Crystallographic Data Centre via www.ccdc.cam.ac.uk/data_request/cif. Supplementary

data associated with this article can be found, in the online version, at doi:10.1016/j.jorganchem.2007.11.028.

References

[1] (a) R.D. Adams, B. Captain, R.H. Herber, M. Johansson, I. Nowik, J.L. Smith Jr., M.D. Smith, Inorg. Chem. 44 (2005) 6346;
(b) R.D. Adams, B. Captain, M. Johansson, J.L. Smith Jr., J. Am. Chem. Soc. 127 (2005) 489.

[2] R.D. Adams, B. Captain, L. Zhu, Inorg. Chem. 44 (2005) 6623.

[3] (a) P. Garrou, Chem. Rev. 85 (1985) 171;
(b) M.I. Bruce, N.N. Zaitseva, B.W. Skelton, A.H. White, J. Organomet. Chem. 515 (1996) 143;
(c) C.W. Bradford, R.S. Nyholm, G.J. Gainsford, J.M. Guss, P.R. Ireland, R. Mason, J. Chem. Soc., Chem. Commun. (1972) 87;
(d) G.J. Gainsford, J.M. Guss, P.R. Ireland, R. Mason, C.W. Bradford, R.S. Nyholm, J. Organomet. Chem. 40 (1972) C70;
(e) A.J. Deeming, S.E. Kabir, M. Underhill, J. Chem. Soc., Dalton Trans. (1973) 2589;
(f) A.J. Deeming, I.P. Rothwell, M.B. Hursthouse, J.D. Backer-Dirks, J. Chem. Soc., Dalton Trans. (1981) 1879;
(g) S.C. Brown, J. Evans, M.J. Webster, J. Chem. Soc., Dalton Trans. (1980) 1021;
(h) R.D. Adams, B. Captain, W. Fu, M.D. Smith, J. Organomet. Chem. 651 (2002) 124.

[4] (a) W.K. Leong, G. Chen, Organometallics 20 (2001) 2280;
(b) W.K. Leong, G. Chen, J. Cluster Sci. 17 (2006) 111.

[5] P.O. Nubel, T.L. Brown, J. Am. Chem. Soc. 106 (1984) 644.

[6] SAINT+, version 6.2a, Bruker Analytical X-ray Systems, Inc., Madison, WI, 2001.

[7] G.M. Sheldrick, SHELXTL, version 6.1, Bruker Analytical X-ray Systems, Inc., Madison, WI, 1997.

[8] M.R. Churchill, K.N. Amoh, H.J. Wasserman, Inorg. Chem. 20 (1981) 1609.

[9] U. Flörke, M. Woyciechowski, H.-J. Haupt, Acta Crystallogr., Sect. C 44 (1988) 2101.

[10] A.H. Klahn, A. Toro, M. Arenas, V. Manriquez, O. Wittke, J. Organomet. Chem. 532 (1997) 39.

[11] D.M. Kimari, Am. Duzs-Moore, J. Cook, K.E. Miller, T.A. Budzichowski, D.M. Ho, S.K. Mandal, Inorg. Chem. Commun. 8 (2005) 14.

[12] G. Albertin, S. Antoniutti, S. Garcia-Fontan, R. Carballo, F. Padoan, J. Chem. Soc., Dalton Trans. (1998) 2071.

[13] U. Florke, H.-J. Haupt, Z. Kristallogr. 209 (1994) 702.

[14] H.-J. Haupt, P. Balsaa, U. Florke, Inorg. Chem. 27 (1988) 280.